CRITICAL HALO LOSS LOCATIONS IN THE LHC

G. Robert-Demolaize, R. Aßmann, C. Bracco, S. Redaelli, T. Weiler, CERN, Geneva, Switzerland

Abstract

Results of simulations with all movable elements of the LHC collimation system [1] are discussed for various operation modes. Compared to previous results, the placing of additional collimators reduced the beam losses by a factor 10 in the ideal machine case, i.e. nominal collimators settings for both 450 GeV and 7 TeV beam energies. First results for Beam 2 are also reviewed. The sensitivity of the system to free orbit oscillations is addressed. These results show that it is sufficient to use a limited number of beam loss monitors (BLMs) for the setup and optimization of the LHC Collimation System.

INTRODUCTION

The LHC collimators located in the two warm insertions dedicated for beam cleaning are used to intercept beam halo. A small fraction of the halo leaks out and gets lost at characterisitc locations around the ring. The performance of the system is described by its *local cleaning inefficiency*:

$$\eta = \frac{\text{number of protons lost in the machine aperture}}{\text{number of protons absorbed by the system} \times \Delta L} \ ,$$

with ΔL a given length over which losses are distributed, which will be 10 cm in the following. Critical loss locations are spotted by comparing the local inefficiency values with the magnet quench levels for estimated minimal beam lifetimes [2, 3]. Simulations are first done for nominal machine optics. Afterwards error models are applied. The nominal reference cases are defined with the parameters listed in Tables 1 and 2.

Table 1: Optics parameters of the simulated nominal cases.

Case	E [TeV]	IR 1 & 5	IR 2 & 8
Injection	0.45	$\beta^* = 17$ m	$\beta^* = 10$ m
Collision	7	$\beta^* = 0.55$ m	$\beta^* = 10$ m

Table 2: Minimal beam lifetimes τ and corresponding required local inefficiencies for the simulated nominal cases at the quench limit.

Case	τ [h]	η_{quench} [m^{-1}]
Injection	0.1	10^{-3}
Collision	0.2	2×10^{-5}

These LHC optics are then used for studies of horizontal and vertical halo cases, usually tracked separately. A description of the tracking tools can be found in [4, 5].

To monitor and control the losses, about 3700 BLMs are being installed in the LHC for the two beam lines. In the early stages of machine commissioning, the full set of BLM information may not be required. Identifying the BLM channels needed for early operation requires the study of loss locations. This paper presents the results for beam halo tracking considering various ideal and error scenarios for both Beam 1 and Beam 2 and for the betatron cleaning insertion. A list of critical loss locations is introduced as a baseline for a minimum workable BLM system for commissionning and early operations of the LHC collimation system.

SCENARIOS FOR HALO TRACKING

In addition to the ideal case, a horizontal beam halo with a free closed orbit oscillation in the horizontal plane is considered. To take into account all possible cases for the error both in phases and amplitudes, two horizontal kickers were selected, separated by a phase advance of $\frac{\pi}{2}$ to allow a full phase scan within $[-\pi, \pi]$. The worst phase is found by observing the most critical loss location, i.e. where the largest number of losses occur. Once this phase is found, a scan in error amplitude for that phase is performed.

This whole process (phase + amplitude) is done following a *static situation*: all collimators are recentered around the perturbed closed orbit and the amplitude of the error reaches the estimated tolerances of each operational mode. For the nominal optics described in Table 1, the closed orbit tolerances correspond to a $\pm$ 4 mm perturbation anywhere in the machine except in the collision energy case for which the tolerances are reduced to $\pm$ 3 mm in the insertion regions[1].

CRITICAL LOCATIONS FROM BEAM LOSS PATTERNS

Loss maps are obtained for the nominal and error scenarios described above. In the following, locations labeled as cold losses correspond to cold elements of the machine in which protons are lost. Following the same principle, losses happening in warm elements are labeled as warm losses.

By comparing the ideal machine patterns with the perturbed cases, one can spot the critical loss locations in the superconducting regions of the machine.

---

[1] For aperture calculations, tolerances are reduced to $\pm$ 3 mm everywhere in the machine in the collision energy case

Closed orbit error - injection optics

The observations shown in [6] for Beam 1 are valid for Beam 2 as well. A closed orbit perturbation of 4 mm at injection optics induces a loss of a factor 2 in cleaning efficiency at the worst phase location and the loss locations are identical between the ideal and the perturbed case downstream of IR7 (Fig. 1 and 2). The first high loss locations correspond to the first two high dispersion locations, at the end of the dispersion suppressor.
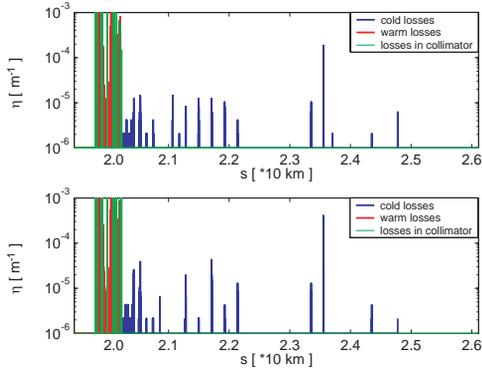

Figure 1: Beam 1 loss patterns for injection optics from the start of IR7 to the end of arc 8-1 for an ideal machine (top) and a $\pm$ 4 mm horizontal orbit perturbation (bottom). The quench level is 10^{-3} protons.m^{-1}. Beam 1 goes from left to right.
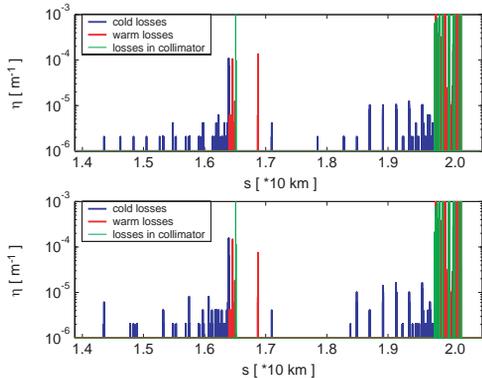

Figure 2: Beam 2 loss patterns for injection optics from the end of arc 5-6 to the end of IR7 for an ideal machine (top) and a $\pm$ 4 mm horizontal orbit perturbation (bottom). The quench level is 10^{-3} protons.m^{-1}. Beam 2 goes from right to left.

Losses in the dispersion suppressor cannot be avoided: off-momentum halo is generated at the collimators due to single-diffractive scattering during the interaction between an incoming proton and the collimator material. Protons with large energy spread are likely to get lost at the first high dispersion location. This defines a characteristic location for proton losses, and sets at the same time a fundamental limitation to the betatron cleaning efficiency.

Closed orbit error - collision optics

At collision optics, one can count less loss locations along the machine compared to the injection optics case

but at the same time more peaks are getting closer to the quench limit. When comparing the ideal machine case with the case of an orbit error, it can be seen in figure 3 and 4 that the cleaning system looses up to a factor 2.4 in efficiency for Beam 2.
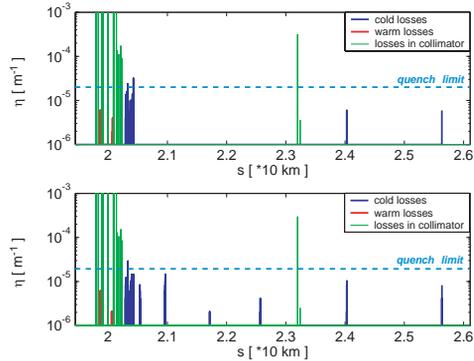

Figure 3: Beam 1 loss patterns for collision optics from the start of IR7 to the end of arc 8-1 for an ideal machine (top) and a horizontal orbit perturbation of $\pm$ 4 mm in the arcs and $\pm$ 3 mm in the insertion regions (bottom). Beam 1 goes from left to right.
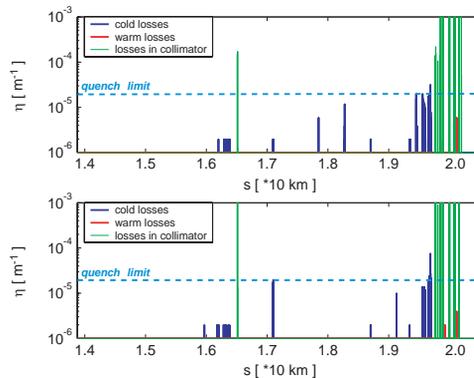

Figure 4: Beam 2 loss patterns for collision optics from the end of arc 5-6 to the end of IR7 for an ideal machine (top) and a horizontal orbit perturbation of $\pm$ 4 mm in the arcs and $\pm$ 3 mm in the insertion regions (bottom). Beam 2 goes from right to left.

Downstream of IR7, it can be seen that the main loss locations are mostly identical for the ideal and the perturbed case. It can also be seen that most of the peaks showing up in the perturbed case correspond to critical locations already spotted in the injection case.

Summary

Scanning all phases and amplitudes, it was possible to identify 43 critical loss locations for injection and 29 for collision considering the betatron cleaning insertion only. This sums up to 59 different locations that systematically show loss peaks, 13 elements being critical for both energies. These 13 locations correspond to the end of the dispersion suppressor of IR7 and the arc downstream. Tables 3 and 4 summarize the predicted locations for "golden" BLMs, i.e. characteristic loss locations due to collimation,

to which locations of collimators should be added. It is suggested that a possibly reduced BLM system should at least cover these locations for an efficient quench protection in various machine operation with error scenarios.

BLMs at similar locations around IR3 and at the triplet magnets must be added. Energy deposition studies are performed in parallel to check the influence of particle showers originating from the tertiary collimators (TCT) protecting the triplet magnets close to the experimental insertions.

Table 3: Critical loss locations at injection optics without momentum cleaning.

Beam 1		Beam 2	
Q11.R3		Q28.R3	Q11.R6
DFBA.R6		Q18.L4	Q31.L7
MB9.R7		Q10.L4	Q27.L7
MB11.R7		Q22.R5	Q23.L7
Q11.R7		Q28.L6	Q19.L7
MB13.R7		MB28.L6	MB19.L7
Q13.R7		Q25.L6	Q15.L7
Q23.R7		Q20.L6	MB15.L7
Q27.R7		MB20.L6	Q11.L7
Q31.R7		MB16.L6	MB11.L7
Q33.L8		MB14.L6	MB9.L7
Q29.L8		MB12.L6	Q8.L7
Q25.L8		MB9.L6	MB8.L7
Q2.R8		MB8.L6	
Q6.R8		Q4.L6	

Table 4: Critical loss locations at collision optics without momentum cleaning.

Beam 1		Beam 2	
Q6.L3	Q21.R7	Q11.R6	Q9.L7
Q8.R7	MB34.L8	MB12.R6	MB9.L7
MB9.R7	Q33.L8	Q25.R6	Q8.L7
Q9.R7	Q25.L8	Q33.R6	MB8.L7
Q10.R7	Q17.L8	Q19.L7	
MB11.R7	Q16.R8	Q13.L7	
Q11.R7	Q30.R8	MB13.L7	
Q13.R7	Q22.L1	Q11.L7	
MB21.R7		MB11.L7	

The tracking tools also allow checking the longitudinal distribution of losses over any magnetic element. The planned positions of the BLM system for each element is shown in Fig. 5, which also includes the longitudinal distribution of losses along the considered magnet. It can be seen that it would be sufficient to use the channels from the first 2 BLMs at a quadrupole since the losses appear to be concentrated at the beginning of the element (see also [7] for more details).

CONCLUSION

The response of the LHC collimation system to free orbit oscillations for Beam 1 and Beam 2 has been reviewed.
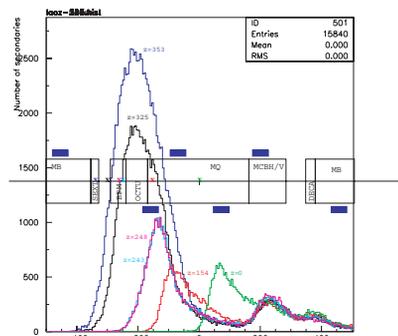

Figure 5: Shower development in the cryostat of a quadrupole. The positioning of the detectors (blue boxes) has been optimized to catch losses (colored curves) and to minimize uncertainty of ratio of energy deposition in coil and detector (courtesy of L. Ponce).

With the specified LHC orbit errors, critical locations along the machine can be identified and used to define a minimum workable BLM system for the commissioning and set-up of the collimators during the early stages of operation. Some locations are critical for both 450 GeV and 7 TeV. The dispersion suppressor immediately downstream of IP7 is the most critical region of the machine, with many losses concentrated over a few elements (the equivalent of two cells of the lattice). Energy deposition studies are ongoing for particle showers generated by inelastic proton-matter interaction in the tertiary collimators (close to the triplet magnets) and downstream of the beam dump protection equipment (TCDQ).

Further studies are planned to obtain loss maps for beta-beating errors, tables of magnetic field errors for the dipoles, alignment errors for magnets in the aperture models and error scenarios for the mechanical parameters of the collimators (e.g. longitudinal tilt angle of one jaw).

REFERENCES

[1] "LHC Design Report", Volume I, Ch. 18, CERN-2004-003.

[2] R. Aßmann: "Collimators and cleaning: could this limit the LHC performance ?", Proc. Chamonix 2003, CERN-AB-2003-008, pp. 163-170.

[3] J.B. Jeanneret, D. Leroy, L. Oberli, T. Trenckler: "Quench levels and transient beam losses in the LHC magnets", CERN-LHC-PROJECT-REPORT-44, 1996.

[4] G. Robert-Demolaize, R. Aßmann, S. Redaelli, F. Schmidt: "A new version of SixTrack with collimation and aperture interface", Proc. PAC 2005, CERN-AB-2005-033.

[5] S. Redaelli: "LHC aperture and commissioning of the collimation system", Proc. Chamonix 2005, CERN-AB-2005-014, pp. 268-277.

[6] G. Robert-Demolaize, R. Aßmann, C. Bracco, S. Redaelli, T. Weiler: "Critical beam losses during commissioning and initial operation of the LHC", Proc. Chamonix 2006, CERN-AB-2006-014, pp. 109-116.

[7] B. Dehning: "Commissioning of beam loss monitors", Proc. Chamonix 2006, CERN-AB-2006-014, pp. 117-119.